


PAPER



Cite this: *Polym. Chem.*, 2019, **10**, 3097

Selective or living organopolymerization of a six-five bicyclic lactone to produce fully recyclable polyesters†

Robin M. Cywar,  Jian-Bo Zhu and Eugene Y.-X. Chen  *

Organocatalyzed ring-opening polymerization (O-ROP) of a six-five bicyclic lactone, 4,5-*trans*-cyclohexyl-fused γ -butyrolactone (4,5-T6GBL), can be topologically selective or living at room temperature, depending on catalyst structure. A screening of (thio)urea [(T)U] and organic base pairs revealed unique trends in reactivity for this monomer as well as the most active catalyst pairs, which were employed as received commercially to produce relatively high molecular weight (M_n up to 106 kDa), low dispersity ($D = 1.04$) linear poly(4,5-T6GBL) in a living fashion. The ROP using a hybrid organic/inorganic pair of TU/KOMe in neat conditions led to poly(4,5-T6GBL) with even higher molecular weight ($M_n = 215$ kDa, $D = 1.04$). In comparison to the metal-catalyzed system, (T)U-base pairs exhibited competitive kinetics and reached higher monomer conversions, and their reactions can be performed in air. In addition, the resulting polymers required less purification to produce materials with higher onset decomposition temperature. (T)U-base pairs were selective towards linear polymerization only, whereas triazabicyclodecene can catalyze both polymerization and (quantitative) depolymerization processes, depending on reaction conditions. Cyclic polymers with $M_n = 41$ –72 kDa were selectively formed *via* N-heterocyclic carbene-mediated zwitterionic O-ROP.

Received 6th February 2019,
Accepted 27th March 2019

DOI: 10.1039/c9py00190e

rsc.li/polymers

Department of Chemistry, Colorado State University, Fort Collins, CO 80523-1872, USA. E-mail: eugene.chen@colostate.edu; Fax: (+1) 970-491-1801

† Electronic supplementary information (ESI) available: Additional details and characterization data. See DOI: 10.1039/c9py00190e



Eugene Y.-X. Chen

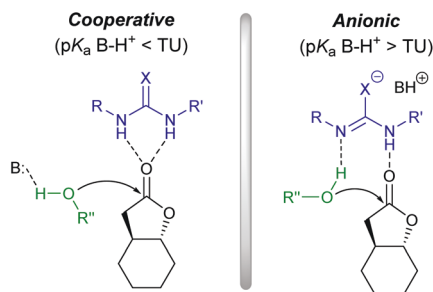
Eugene Chen came to the United States for graduate studies from China in 1991 and received his Ph.D. degree from The University of Massachusetts, Amherst, in 1995, under the direction of late Professors James Chien and Marvin Rausch. After a postdoctoral stint at Northwestern University with Professor Tobin Marks, he joined The Dow Chemical Company in late 1997, where he was promoted from Sr. Research Chemist to Project

Leader. He moved to Colorado State University in August 2000, where currently he is the John K. Stille Endowed Chair in Chemistry and the Millennial Professor of Polymer Science & Sustainability. His research interests encompass broadly the areas of polymer science, green & sustainable chemistry, and catalysis.

1. Introduction

Organocatalysis for small molecule and polymer synthesis has evolved steadily over the past two decades, notably in the field of ring-opening polymerization (ROP) of heterocyclic monomers.^{1–20} The use of organic catalysts has demonstrated certain advantages spanning convenience, economics, environmental concerns, and materials applications.^{1,4–6,9} Not only are organocatalysts considered a sustainable alternative to organometallic complexes¹ for both polymerization and depolymerization,²¹ but their use can also enable polymer applications where metal residues are undesired, such as in biomedical, electronic, and food packaging fields.^{4–6,9}

(Thio)urea [(T)U] species have proved to be highly effective catalysts for organocatalyzed ROP (O-ROP), touting similar or better performance than metal-based catalysts towards the ROP of classical strained rings (*e.g.* lactones and lactide) in terms of kinetics and selectivity.^{8,14–16} (T)U species catalyze living polymerizations with remarkable selectivity towards polymerization over transesterification (chain transfer), and the mechanism can be modulated by balancing the acidity of the (T)U and the basicity of a co-catalyst.¹⁶ A base that is too weak to deprotonate the (T)U will promote a neutral, ‘cooperative’ mechanism while a stronger organic or alkoxide base will generate a catalytic (T)U anion (Scheme 1). This mechanistic handle, created by the tunable acidity of the (T)U and selection



Scheme 1 Proposed (T)U modes of action in ROP of 4,5-T6GBL.

of commercially available bases, provides a framework for the rational catalyst design employed in recent works as well as this study. New advancements in (T)U catalysis include the bulk polymerization of γ -butyrolactone (GBL) to relatively high molecular weights and the synthesis of stereoregular polyesters, achieved through clever catalyst design to minimize competitive epimerization pathways.^{22–25} While (T)U-based catalysts are selective towards the formation of linear polymers, the ability to selectively form cyclic polymers is also desirable.²⁶ In this context, N-heterocyclic carbenes (NHCs) produce macrocyclic polyesters free of linear chains *via* zwitterionic ring-opening polymerization (ZROP).^{26–28} In the absence of initiator, NHCs behave as strong nucleophiles towards lactones, but poor leaving groups in the resulting tetrahedral intermediate. These characteristics, coupled with fast propagation relative to initiation and cyclization, allow relatively high molecular weight cyclic polymers to form regardless of the monomer-to-initiator ratio ($[M]/[I]$).²⁶

The need to combat the plastic waste issues that threaten the environment and cause enormous materials value loss to the economy has opened many new avenues in polymer synthesis and degradation research.^{19,21,29–40} While viable strategies are being developed to degrade or upcycle pollutant commodity plastics, the transition to a circular plastics economy calls for the innovative design of new materials with ‘built-in’ recyclability.^{41,42} The non-strained GBL is intrinsically depolymerizable (*i.e.*, chemically recyclable) due to a low ceiling temperature (T_c), but consequently its polymer, P(GBL), can only be produced at sub-zero temperatures and possesses limited thermostability.^{19,33} Recent developments in GBL-derivatives have allowed polymerization at room temperature, in addition to enhanced materials properties.^{35,36} Fusion of an additional ring to the GBL core increases the ring strain, effectively driving the ROP process forward while maintaining complete chemical recyclability of the resulting polymer. When a *trans*-cyclohexane ring is fused at the β,γ (4,5) carbons of GBL, the ring strain energy (ΔH_p°) increases significantly from -5.4 kJ mol^{-1} (GBL) to -18 kJ mol^{-1} (4,5-T6GBL).⁴³ As a result, T_c is also drastically raised. With this shift, ambient temperature is now far below the T_c and polymerization can proceed smoothly to high conversions at 25 °C.

Recently, we polymerized 4,5-T6GBL by metal-catalyzed coordination ROP, which produced amorphous P(4,5-T6GBL)

with M_n up to 89 kDa and a glass-transition temperature (T_g) of 75 °C, intriguingly similar to that of poly(ethylene terephthalate) (PET).³⁶ The constitutional isomer 3,4-T6GBL can be polymerized to a polymer with M_n exceeding $1 \times 10^6 \text{ Da}$ by a yttrium complex, but the presence of an acidic proton α to the carbonyl at the fusion point of the GBL ring hinders O-ROP by basic catalysts due to rapid isomerization to the non-polymerizable *cis* isomer.³⁵ Here, we report the O-ROP of 4,5-T6GBL, a new monomer in the O-ROP space, to linear and cyclic polymers selectively, as well as the quantitative depolymerization with an organic catalyst. Although both metal and organocatalyzed systems are of a living nature and produce polymers of similar M_n and narrow dispersity on a similar timescale, the organic system reported herein demonstrated several advantages including: (1) higher monomer conversions, (2) reduced polymer purification requirements, (3) increased onset decomposition temperature (T_d), and (4) air stability.

2. Results and discussion

2.1. Synthesis of linear P(4,5-T6GBL) *via* O-ROP

2.1.1 Initial organocatalyst screening. Monomer 4,5-T6GBL, although polymerizable even at room temperature, is still significantly less strained (by more than 4 kJ mol^{-1}) than classical 6 and 7-membered lactones and lactide (see Table S1† for ΔH_p° values). The ROP of 4,5-T6GBL by classic anionic initiators produced low molecular weight oligomers with M_n up to only 6.2 kDa (by gel-permeation chromatography, GPC) or 2.6 kDa (by NMR).⁴³ Considering a myriad of organocatalysts available for ROP,² we began our O-ROP study by probing some of the most effective catalyst families for activity and selectivity towards 4,5-T6GBL, which requires powerful catalysts/initiators to render its effective polymerization. We hypothesized that activation of an alcohol initiator alone (by a base) may not be sufficient to afford higher M_n polymers. Likewise, monomer activation alone (by protic acids) may not be sufficient, but *dual activation* could provide the necessary electron deficiency at the monomer carbonyl coupled with increased nucleophilicity of an activated alcohol initiator.² This hypothesis appeared to be correct, as only the bifunctional TU and triazabicyclodecene (TBD) catalysts showed promising preliminary results (Table 1). For example, TBD/BnOH mediated well-controlled polymerization, affording a polymer with $M_n = 9.14 \text{ kDa}$, initiation efficiency (I^*) = 99%, and $D = 1.11$ (run 7). However, because this equilibrium polymerization is limited to high monomer concentration conditions⁴⁴ and TBD does not offer tunability, we extended the investigation by exploring (T)U catalysis. Inspired by Waymouth’s recent study,¹⁶ we screened a matrix of three TU catalysts and three U catalysts (structures shown in Fig. 1A) with three different bases (1,8-diazabicyclo[5.4.0]undec-7-ene, DBU; 2-*tert*-butylimino-2-diethylamino-1,3-dimethylperhydro-1,3,2-diazaphosphorine, BEMP; and 1,3-dimesitylimidazol-2-ylidene, IMes). The combination of each (T)U with each base provides different mechanistic scenarios where there is a mis-

Table 1 Initial screening of organocatalyst families

Run	Cat.	I	[M]/[Cat.]/[I]	Solvent	Time (h)	Conv. (%)
1	DPP	Ph ₂ CHCH ₂ OH	50/1/1	Neat	24	2
2	^t Bu-P ₄	Ph ₂ CHCH ₂ OH	50/1/1	Neat	24	5
3	TfOH	BnOH	100/1/1	Neat	24	0
4	TU-2	NaOMe	100/3/1	Neat	12	53
5	TU-2	NaOMe	100/3/1	THF(5 M)	36	26
6	TBD	Ph ₂ CHCH ₂ OH	50/1/1	Neat	16	50
7	TBD	BnOH	100/2.5/1	Neat	48	64

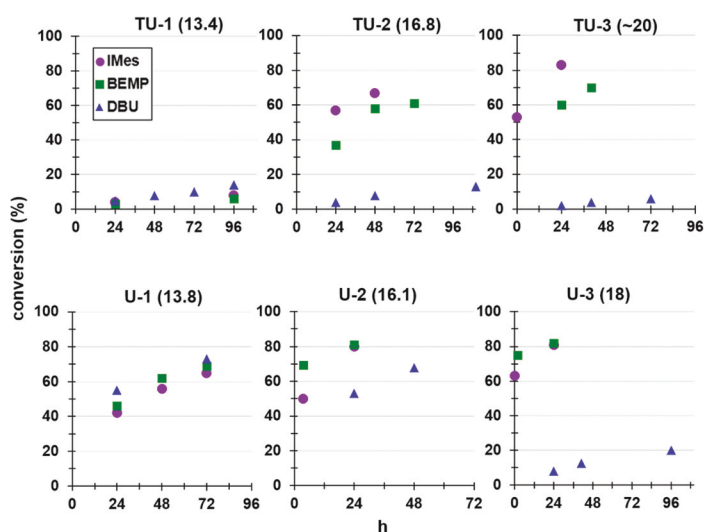
A

	TU	TU-1	TU-2	TU-3
Base	pK _a	13.4	16.8	~20
DBU	13.9	14%	13%	6%
BEMP	16.5	6%	61% 7.70 kDa, \bar{D} = 1.04	70% 8.22 kDa, \bar{D} = 1.04
IMes	18-24	8%	67% 9.06 kDa, \bar{D} = 1.08	83% 10.8 kDa, \bar{D} = 1.11

	U	U-1	U-2	U-3
Base	pK _a	13.8	16.1	18.7
DBU	13.9	73% 8.14 kDa, \bar{D} = 1.08	68% 7.08 kDa, \bar{D} = 1.08	20% 3.56 kDa, \bar{D} = 1.40
BEMP	16.5	69% 7.45 kDa, \bar{D} = 1.07	81% 9.74 kDa, \bar{D} = 1.10	82% 10.1 kDa, \bar{D} = 1.09
IMes	18-24	65% 5.88 kDa, \bar{D} = 1.08	80% 10.2 kDa, \bar{D} = 1.11	81% 9.50 kDa, \bar{D} = 1.12

no gelation occurred
 gelation within 24h
 gelation within few hours or minutes

B

Fig. 1 General results and trends obtained from (T)U/organic base screening: maximum conversion, M_n , and \bar{D} in a matrix presentation (A) and kinetic profiles in time-conversion plots (B).

match in each direction ($pK_a(\text{T)U} > \text{BH}^+$, cooperative mechanism; $pK_a(\text{T)U} < \text{BH}^+$, anionic mechanism, Scheme 1) in addition to a matched acidity case. The well-matched pairs were predicted to have the highest activity,¹⁷ likely due to effective buffering of the highly basic alkoxide chain end.^{16,22}

For this initial (T)U/base screening, the monomer conversion was measured at the gel point, but the reaction was allowed to continue for 24 h (or longer for slower systems) to reach maximum conversion. The results in Fig. 1 (tabulated results can be found in Table S2†) revealed trends consistent with previous findings regarding (T)U activity^{14–16} as well as unique trends in activity for this monomer. Generally, the matched pK_a cases had the highest activity, higher pK_a (T)U's were most active, and ureas were more active than thioureas with similar pK_a 's (Fig. 1). Ureas were also more active than TU's with the same substituents: the TU analog of U-1 (pK_a 8.5) resulted in only 10% conversion after 120 h when deprotonated with IMes, while U-1/IMes reached 65% conversion in 72 h. Two catalyst pairs, TU-3/IMes and U-3/IMes, gelled in just one min and led to the highest conversions, thus standing out as the optimal catalyst pairs to employ for subsequent higher degree of polymerization (DP) runs. These structures

were the weakest acids and therefore their anionic, conjugate base forms are the strongest bases; this trend is also consistent with the requirement of high- pK_a (T)U anions for GBL polymerization.^{22,24} TU-3/IMes was also robust enough to catalyze the polymerization *in air* with equal performance as that performed under nitrogen (Table S2†). In fact, the dispersities of duplicate in-air runs were closer to 1.00 and the measured M_n values even closer to the theoretical M_n than for the run performed inside the glovebox ($I^* = 92$ or 98 vs. 108%), although likely due to quenching the reaction at 6.5 h rather than 24. While (T)U catalysts are selective towards monomer addition over chain transfer,^{14,15} transesterification could be exacerbated in the gel phase due to limited monomer mobility and close proximity of open-chain ester bonds. As conversion increased, the phase was observed to progress from a viscous fluid to a glassy, impenetrable solid.

Data from this initial screening provided additional insights to the nature of this monomer system. Distinct sensitivities to base strength were observed among the 6 (T)U catalysts when conversion vs. time was plotted for all aliquots taken during the screening runs (Fig. 1B). The urea species displayed much less base sensitivity, generally leading to at least

70% conversion even if slow, while only two TU species reached over 70% conversion. TU-1 and U-1 showed completely opposite activities despite their similar pK_a , and U-2 (pK_a 16.1) still led to 68% conversion after 48 h even when paired with DBU (pK_a 13.9), whereas TU-2 (pK_a 16.8) with DBU largely failed (13% conversion after 96 h). These distinctions can be explained by neutral urea species acting as stronger H-bond donors than TU's (even if their pK_a values are equal),⁴⁵ and by urea anions acting as stronger bases than TU anions. A neutral TU may be a less effective hydrogen bond donor than a neutral urea with the same substituents or pK_a due to overlap with the large electron cloud of the sulfur atom but is an apparent stronger acid due to increased conjugate base stability. In the anionic form, the large sulfur atom can better stabilize the negative charge, therefore electron density on the basic nitrogen is diminished as compared to a urea anion. U-2 could participate in a cooperative mechanism with DBU because the H-bonding provided by the neutral urea was sufficient to activate the monomer, whereas TU-2 was unsuccessful in this mode. In the case of TU-1 vs. U-1 (pK_a 13.4 and 13.8, respectively) where at least 50% (T)U anion should have been present with each base, TU-1 was unable to drive polymerization in any scenario while U-1 could, signifying the TU was ineffective in both the neutral and anionic forms. For both TU-3 and U-3, a matched or stronger base was effective for the polymerization, but DBU was not. Being such weak acids ($pK_a > 18$), electrophilic activation of the monomer coupled with the weakest base to activate the alcohol in a cooperative mechanism was not feasible. While neither was successful, U-3 still reached 20% conversion as compared to only 6% for TU-3, once again highlighting urea species' greater H-bond donating ability. It is worth noting here that all mechanistic scenarios can successfully ring-open polymerize more strained monomers such as lactide (LA) and δ -valerolactone (δ -VL) if given enough time to reach completion.¹⁶

2.1.2 Preparation of higher M_n polymers with TU-3/IMes. With the two fastest catalyst pairs [(T)U-3/IMes] in hand, the

target DP was raised to 200. Trials with U-3/IMes appeared to suffer a lack of control upon increasing the $[M]/[I]$ ratio, and the resulting polymer M_n values were much lower than expected from the $[M]/[I]$ (Table S4†). The I^* values were correspondingly high: 180–223% for a $[M]/[I]$ ratio of 200 and 267% for a $[M]/[I]$ ratio of 500. The U-3/IMes pair was thus abandoned, and higher $[M]/[I]$ ratio trials were continued with TU-3/IMes as this pair displayed greater control over the polymerization with M_n values more closely matched to that predicted by the $[M]/[I]$ ratio (Table 2).

Because (T)U-catalyzed ROPs are known to follow first-order kinetics in both monomer and catalyst concentrations,^{14–16} we kept the catalyst concentration at approximately 1 mol% for neat runs and 2 mol% when solvent was used. However, runs with 0.5 mol% or less were still successful on a reasonable timescale (6–24 h, Table 2, runs 4 and 9). Using an excess of TU to IMes did not appear to affect the polymerization appreciably (Table 2, run 4 vs. run 1), with both conditions producing P(4,5-T6GBL) with essentially quantitative I^* (101–104%) and extremely low D (1.02) values. When tetrahydrofuran (THF) or toluene (Tol) were used at the 200 ratio, the equilibrium was reached in 3–5 h, however, at the expense of lower conversion and thus M_n values. At this ratio, THF led to a relatively broad dispersity of 1.13, and stirring for 24 h led to a more severe broadening to a D of 1.21 and reduced I^* (70%). Even a high monomer concentration of 5.0 M limited maximum conversion at room temperature due to the proportional relationship of the polymerization T_c and $[M]$.⁴⁴ For example, when an equilibrated reaction (200/5/5/1, 5.0 M Tol) was moved to a -30°C environment, the equilibrium conversion increased from 62 to 86%. Overall, the use of solvent had no appreciably positive effect on the polymerization (Table 2, runs 2, 3, 7, and 8).

Above target DP500, the I^* value departed from unity (Table 2, runs 5–11), but the polymerization remained well controlled ($I^* < 150\%$, $D \leq 1.06$) through target DP1000. This phenomenon was also observed in the metal-catalyzed ROP of 4,5-T6GBL, but this organocatalyzed system consistently

Table 2 Selected results of polymerization catalyzed by TU-3/IMes

Run	$[M]/[TU-3]/[IMes]/[I]$	Solvent	Time (h)	Conv. ^a (%)	$M_{n, \text{GPC}}^b$ (kg mol ⁻¹)	$M_{n, \text{theor.}}^c$ (kg mol ⁻¹)	$I^*{}^d$ (%)	D^b (M_w/M_n)
1	200/2.5/2.5/1	Neat	24	79	21.1	22.0	104	1.02
2	200/5/5/1	Tol 5M	4	61	18.1	17.2	96	1.05
3	200/5/5/1	THF 5M	3	47	13.7	13.7	100	1.13
4 ^e	250/3/1/1	Neat	6	74	26.4	26.5	101	1.02
5	500/5/5/1	Neat	24	76	39.5	53.1	134	1.03
6	500/10/10/1	Neat	6	74	37.4	52.2	140	1.04
7	500/10/10/1	Tol 5 M	10	58	28.6	41.0	143	1.04
8	500/10/10/1	THF 5 M	10	45	23.8	32.7	137	1.06
9 ^e	1000/5/5/1	Neat	18	69	72.6	98.8	136	1.02
10 ^e	1000/10/10/1	Neat	7	69	71.8	98.4	137	1.04
11 ^e	2000/20/20/1	Neat	16.5	72	106	200	189	1.04

All polymerizations performed in N_2 -filled glovebox at ambient temperature with 2 mmol 4,5-T6GBL unless otherwise noted; I = BnOH. ^a Monomer conversion determined by ^1H NMR in CDCl_3 . ^b Number-average molecular weight (M_n) and dispersity index ($D = M_w/M_n$) determined by gel-permeation chromatography (GPC) at 40°C in CHCl_3 coupled with a DAWN HELEOS II multi (18)-angle light scattering detector and an Optilab TrEX dRI detector for absolute molecular weights. ^c Calculated based on: $([M]_0/[I]_0) \times \text{Conv.}\% \times (\text{molecular weight of 4,5-T6GBL}) + (\text{molecular weight of I})$, using exact equivalents of monomer measured. ^d $I^* = (M_{n, \text{theor.}}/M_{n, \text{GPC}}) \times 100$. ^e Runs 4 and 10 used 3 mmol 4,5-T6GBL, run 9 used 4 mmol, and run 11 used 11.5 mmol (1.6 g).

reached higher conversions.³⁶ Although chain-transfer is likely responsible for obtaining M_n values less than theoretical, a concurrent broadening of dispersity was not observed. We hypothesize that the resulting trans-esterified chains remained as active, or 'alive', as those initiated by BnOH and continued to add monomer units from the bulk solution at comparable rates. If higher M_n polymers are desired in a shorter timeframe, the catalyst loading can be increased (Table 2, run 5–6 and 9–11). Although the target DP2000 run gave an I^* value of 189%, it still produced a polymer with $M_n = 106$ kDa and $D = 1.04$ (Table 2, run 11), highlighting the robust nature of this system. In comparison, the metal-catalyzed system employing the $[M]/[I]$ of 2000 afforded a polymer with $M_n = 89$ kDa ($I^* = 173\%$, $D = 1.02$), albeit with a lower catalyst loading (0.05 mol%).³⁶ Thus, metal catalysts are still superior in terms of potency towards ROP of this monomer.

2.1.3 Further evidence for living polymerization behavior.

The results described above and shown in Table 2 and Table S2† indicated the polymerization of 4,5-T6GBL by the (T)U/base systems is of a living nature, consistent with the (T)U-catalyzed ROP of typical monomers.^{8,14–16} The O-ROP of parent monomer GBL is not living, however, due to an additional mode of initiation stemming from an enolized GBL, rather than ring-opening of the first monomer *via* nucleophilic attack by initiator.^{19,24}

Besides reaching M_n values close to those expected from $[M]/[I]$ ratios, coupled with low D values, here we provide three additional lines of evidence to support the characterization of a living polymerization. First, the M_n of the growing chains tracked linearly with monomer conversion as shown in Fig. 2A. A slower catalyst pair, U-2/BEMP, was employed to monitor conversion in a wider timeframe than with TU-3/IMes, which gelled quickly. Plots of conversion *vs.* time and $\ln([M]_0/[M])$ *vs.* time (Fig. 2B and C) displayed typical first-order decay and linear trends, respectively, confirming first-order monomer kinetics.

Second, the matrix-assisted laser desorption/ionization time-of-flight mass spectroscopy (MALDI-TOF MS) chain-end analysis of P(4,5-T6GBL) confirmed the BnO/H moieties remained on the initiating and terminating ends, and thus a linear polymer architecture. The MALDI-TOF MS spectrum of a

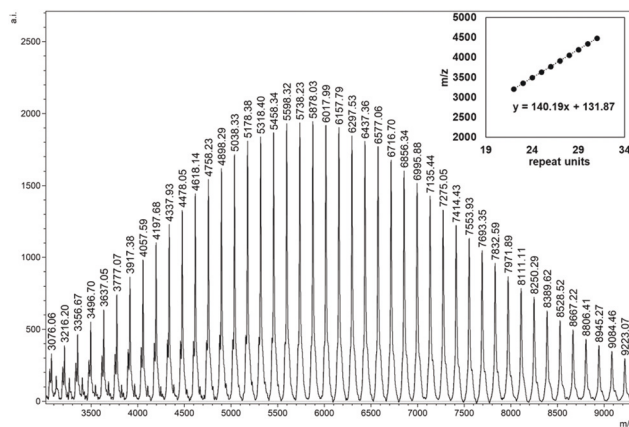


Fig. 3 MALDI-TOF MS spectrum and chain-end analysis of a linear polymer produced by TU-3/BEMP.

low M_n polymer prepared by TU-3/BEMP shows the molecular ion peaks are separated by the mass of one monomer unit (140.18 g mol⁻¹), as indicated by the slope (140.19) of the line created by plotting m/z (y) *vs.* number of repeat monomer units (x) (Fig. 3). The y -intercept corresponds to the mass of the chain ends plus a sodium cation (108.1 + 23.0 g mol⁻¹), and close agreement of the plot value (131.9) to the actual value (131.1) suggests the chain-end fidelity typically associated with living polymerizations. Minor peaks visible in the low molecular weight region represent P(4,5-T6GBL) + H⁺, still carrying BnO/H chain ends.

Third, a chain-extension experiment was performed to produce a block copolymer. L-Lactide (L-LA) was selected as the second block due to its significantly higher activity in the ROP with a catalyst pair of similar basicity;¹⁶ this condition is required to avoid further conversion of 4,5-T6GBL after the second monomer is added and perturbs the equilibrium monomer concentration.³⁶ A ratio of 4,5-T6GBL/TU-3/IMes/BnOH = 200/5/5/1 was employed for the first block, with 5.0 M THF conditions to avoid complete gelling but allow equilibrium to be reached before the addition of L-LA. After 4 h and 48% conversion, a 3.88 M THF solution of L-LA was added and quenched after 10 min. The conversion of L-LA was quantitat-

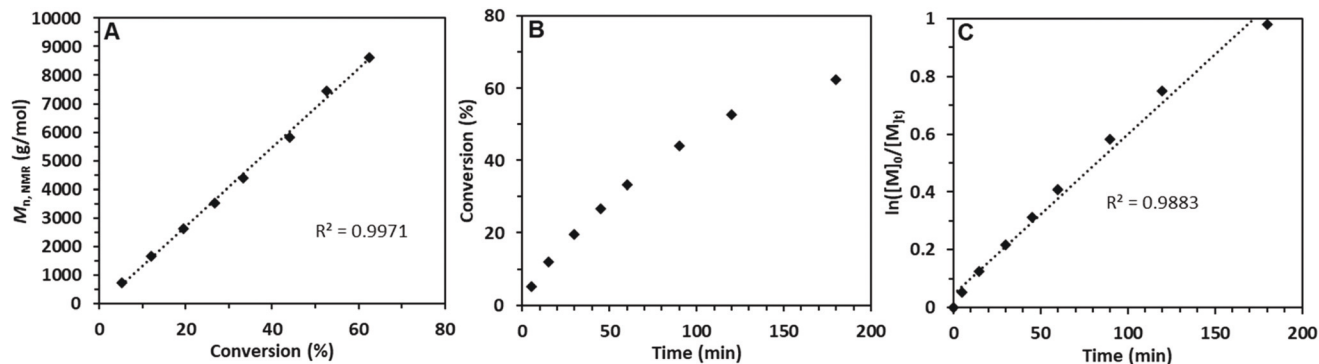


Fig. 2 Kinetic data of P(4,5-T6GBL) synthesis with $[M]/[U-2]/[BEMP]/[BnOH] = 100/2.5/2.5/1$ at 25 °C.

ive while that of 4,5-T6GBL increased by 2%, as opposed to 6% for a trial with ϵ -caprolactone which is less active towards a similar catalyst pair.¹⁶ Although the block copolymer structure was not perfect, the characterization data still showed behaviour consistent with an AB block copolymer (the 2% conversion increase corresponds to only four additional 4,5-T6GBL units incorporated into the PLA block). Additionally, no decrease in P(4,5-T6GBL) conversion after further dilution by the L-LA solution is supportive of the capping of this block by PLA. Fig. S8† shows the GPC elution profiles of the first block and final block copolymer, P(4,5-T6GBL)-*b*-PLA, with differentiated retention times. Differential scanning calorimetry (DSC) analysis (Fig. S12†) displayed two T_g values corresponding to each block: 56 °C for the PLA block and 71 °C for the P(4,5-T6GBL) block. The thermogravimetric (TGA) analysis (Fig. S11†) revealed a single step decomposition ($T_d = 277$ °C, defined by the temperature of 5% weight loss; $T_{max} = 364$ °C, defined by the peak maximum from a derivative (wt%/°C) vs. temperature (°C) plot); a step-wise decomposition of the individual blocks was not observed due to similar T_d values of the respective homopolymers.

The behaviour of this polymerization suggests that the mechanism is in parallel to that of the (T)U catalyzed ROP of typical lactone monomers, which has been studied extensively through kinetic and NMR experiments in addition to computation with density functional theory.^{14,15} Still, there is more to be learned about these intriguing systems, especially in the roles of the cation and reversible chain end protonation. Scheme 2 depicts the proposed mechanism of the ROP catalyzed by TU-3 and IMes, however it should be noted that all possible resonance structures and proton transfers are not shown. There exist many possibilities of proton exchange and

hydrogen bonding among the TU anion, organic cation, and chain end, in addition to resonance within the TU anion. Reversible chain-end protonation has been proposed as a buffering mechanism to reduce the basicity of the alkoxide, which could otherwise be a promiscuous species. When the pK_a of the TU is closely matched with the base, there is an even greater opportunity for this dynamic proton exchange throughout the polymerization.

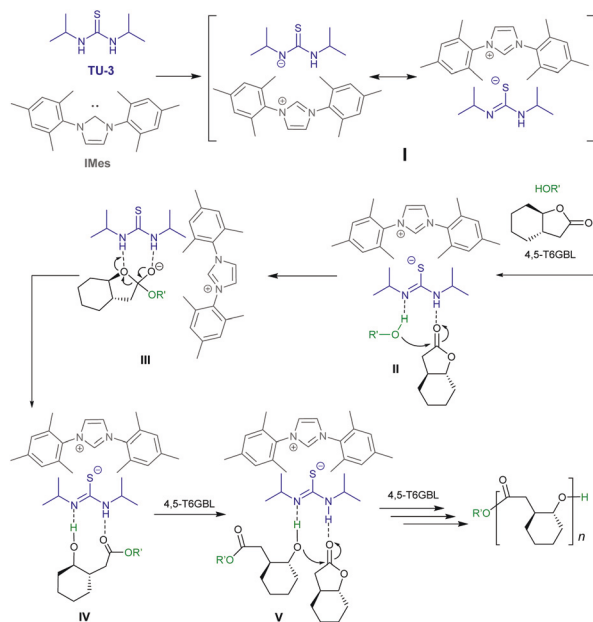
The mechanism presented in Scheme 2 begins with the deprotonation of TU-3 by IMes to form the TU-3 anion and large imidazolium cation. This ion pair (**I**) was typically generated in the presence of monomer and was completely solubilized within 5 min (no reaction ensued until addition of initiator R'OH). Next, the TU-3 anion acts as a bifunctional activator toward both the initiator and monomer, shown in intermediate **II**. Hydrogen bonding of TU-3[−] to the alcohol and hydrogen bond donation to the monomer carbonyl, simultaneously increase the nucleophilicity and electrophilicity, respectively. The bifunctional nature of the catalyst also draws the two activated species close together, facilitating attack on the carbonyl to form tetrahedral intermediate **III** and the subsequent proton transfer to give ring opening product **IV**. Propagation *via* transition state **V** continues with the resulting hydroxy chain end becoming activated for further monomer addition. Because the chain end is nearly always engaged in a hydrogen bond with the TU-anion, its basicity is reduced. Zhang *et al.* suggest this can prevent backbiting in the polymerization of GBL, which could also apply to this system.²²

2.1.4 Polymerizations by TU-3/KOMe and TU-3/KH/MeOH.

Besides the completely organic system, we also investigated the reactivity of TU-3/KOMe systems toward the ROP of 4,5-T6GBL. In these systems, the initiator and base are conveniently packaged into one reagent: methoxide first deprotonates the TU, and the resulting methanol initiator engages in a hydrogen bond with the TU[−]/K⁺ ion pair. An excess of (T)U is typically used to improve the solubility of the complex, while greater excesses can inhibit the polymerization.¹⁵ A nuance of this system with this monomer is that the initiating complex must be formed and completely solubilized before addition of monomer.

Table 3 summarizes selected polymerization results with TU-3/KOMe, which was only successful up to the target DP250. Solution polymerizations exhibited decent control, with $\bar{D} = 1.07$ to 1.16 and $I^* = 91\%$ to 130% (Table 3, runs 1, 3, and 5), but the use of solvent limited monomer conversion and therefore polymer M_n . For run 1, equilibrium was reached in under 10 min, and further stirring of the reaction up to 1 h resulted in no further monomer conversion but a broadening of \bar{D} to 1.30 accompanied with an increase of M_n to 10.8 kDa. A control with only KOMe for the ROP of 4,5-T6GBL was attempted, but prevented by insufficient solubility in THF, toluene, and dichloromethane; in another study, common anionic initiators such as ^tBuOK afforded only low M_n oligomers.⁴³

To conduct TU-3/KOMe runs in neat conditions, the complex was first formed in THF and an aliquot was transferred to the reaction vial. After complete removal of solvent



Scheme 2 Proposed mechanism for the ROP of 4,5-T6GBL by the optimal catalyst pair.

Table 3 Selected results of polymerization catalyzed by TU-3/KOMe and TU-3/KH/MeOH

Run	[M]/[TU-3]/[KOMe]	Solvent	Time (h)	Conv. (%)	M_n , GPC (kg mol ⁻¹)	M_n , theor. (kg mol ⁻¹)	I^* (%)	D (M_w/M_n)
1	100/3/1	THF 5M	10 min	58	8.82	7.99	91	1.16
2	250/3/1	Neat	24	61	73.7	21.7	29	1.10
3	250/3/1	THF 5M	2.5	61	16.4	21.4	130	1.07
4 ^a	250/3/1 (KH)	Neat	6	78	28.0	27.4	98	1.01
5	250/6/1	THF 5M	4.5	53	17.8	18.6	105	1.07
6	250/6/1	Neat	6	58	92.9	20.4	22	1.07
7 ^b	250/6/1	Neat	6	72	137	25.2	18	1.21
8 ^c	250/6/1	Neat	8.5	76	215	26.6	12	1.04

^a This run used KH to form TU anion followed addition of MeOH initiator; 1.3 g 4,5-T6GBL used. ^b This run used 1.5 g (11 mmol) 4,5-T6GBL.

^c This run used 2.5 g (18 mmol) 4,5-T6GBL. See footnotes of Table 2 for explanations and definitions for abbreviations.

in vacuo, the reactor was charged with monomer. Runs 2 and 6–8 in Table 3 present some surprising results of the neat polymerizations. The polymers obtained from these runs had M_n values much higher than expected, >70 kDa for a $[M]/[I]$ of 250, corresponding to low I^* values (12–29%). After monomer addition, the dried-down complexes were observed to dissolve slowly, for example, run 6 took 7 min to become homogeneous, and gelled in about one h. For run 7, which was performed with the same stoichiometry but larger scale, gelling occurred around the same time as homogeneity (25 min) and the resulting M_n was increased to 137 kDa; further scale-up resulted in a polymer of $M_n = 215$ kDa (run 7). The delay in solvation of the catalyst-initiator complex led us to hypothesize that differential initiation was responsible for the unexpectedly high M_n 's. Only a fraction of initiator was introduced to bulk monomer at a given time, leading to a higher effective $[M]/[I]$ in solution. It is also possible that the overall $[I]$ was also reduced during solvent evacuation by evaporation of methanol. Despite this lack of control, D values were still relatively narrow ($D = 1.04$ – 1.21). To test our hypotheses, we performed a control experiment in which the TU anion was solvated by deprotonating with KH in bulk monomer (Table 3, run 4). This solution was homogeneous within 5 min and a sample was taken for ¹H NMR analysis to ensure no monomer conversion occurred. No reaction took place until methanol was added to initiate the polymerization, which afforded a polymer of the expected M_n (28.0 kDa, $I^* = 98\%$) and extremely low dispersity of $D = 1.01$, thus supporting the differential initiation and evaporation hypotheses, which are likely both contributing factors to a higher effective $[M]/[I]$, and which appeared to increase further with scale ($[M]$). Increased broadness in comparison to the KH control and the TU-3/IMes system could be due to the introduction of more initiator to an active polymerization, in which it acts as a chain transfer agent or initiates new chains with limited growth.

Overall, the results presented in Tables 2 and 3 demonstrated four main strategies to obtain P(4,5-T6GBL). First, the TU-3/IMes pair offers an entirely metal-free, living polymerization to obtain relatively high M_n polymers in a reasonable timeframe. Second, the organic/inorganic TU/KOMe system is also effective and is more economical than the use of IMes. Equilibrium is reached quickly, but the requirement to

perform the ROP in solution limits the monomer conversion and polymer M_n . Third, the TU/KH/MeOH system allowed the well-controlled bulk ROP, achieving relatively high monomer conversion of 78% and producing P(4,5-T6GBL) with essentially quantitative efficiency ($I^* = 98\%$) and near unity dispersity ($D = 1.01$). Fourth, the neat KOMe method offers a convenient and economical way to obtain high M_n polymers, however the resulting M_n cannot be predicted by $[M]/[I]$ ratios. Advantages of the TU-3/IMes system include better catalyst/initiator solubility and the ability to modulate the concentration of active TU anion relative to initiator. In the TU-3/KOMe system, the concentration of TU anion is always equivalent to the alkoxide initiator. Additionally, the use of potassium could be undesired for certain polymer applications.

2.2. Synthesis of cyclic P(4,5-T6GBL) by NHC catalysts

Next, we turned our attention to the selective synthesis of polymers with a cyclic topology *via* NHC catalysis. NHC-mediated ZROP has proven to be a powerful method to synthesize cyclic polymers from strained lactones, showing its effectiveness towards 4,5-T6GBL as well. Table 4 summarizes the selected results of polymerizations catalyzed by three NHCs of varying nucleophilicity. IMes is the least nucleophilic of the series and did not initiate the polymerization, whereas 1,3-di-*tert*-butylimidazol-2-ylidene (I^tBu) and 1,3-diisopropylimidazol-2-ylidene (IⁱPr) were effective catalysts. IⁱPr is more nucleophilic than I^tBu, which could account for the markedly higher conversion provided by IⁱPr (74 vs. 56%). The NHC nucleophilicity did not appear to affect the resulting M_n , however (Table 4, run 3 vs. 4).

Table 4 Selected results of NHC catalyzed ZROP

Run	NHC	[M]/[NHC]	Time (h)	Conv. (%)	M_n , GPC (kg mol ⁻¹)	D (M_w/M_n)
1	IMes	100/1	24	0	—	—
2	I ^t Bu	50/1	24	68	45.9	1.30
3	I ^t Bu	100/1	24	56	40.6	1.21
4	I ⁱ Pr	100/1	24	74	42.2	1.38
5	I ⁱ Pr	500/1	50	64	72.1	1.28

Run 4 used 3 mmol 4,5-T6GBL and run 5 used 10 mmol. See footnotes of Table 2 for explanations and definitions for abbreviations.

As expected, polymer M_n values could not be predicted or controlled, but appeared to cyclize after a certain DP (~ 300) had been reached; this lack of control also led to broader dispersity ($D > 1.2$). On the other hand, a higher than average DP of ~ 510 ($M_n = 72.1$ kDa) was obtained by using a significantly higher $[M]/[NHC]$ ratio of 500 on a larger scale (Table 4, run 5 vs. 4).

The obtained polymers were confirmed to be cyclic by the absence of end groups in the NMR spectra (Fig. S13 and S14[†]), and chain-end analysis of the MALDI-TOF MS spectrum (Fig. S18[†]) gave a y-intercept (23.7) corresponding to the mass of only a sodium ion and slope of 140.4, indicating the polymer with no end groups. Additionally, cyclic and linear polymers of similar M_n (42.2 and 39.5 kDa, respectively) had a difference of almost two min in the start of elution off the GPC column. The mechanism for the ZROP of 4,5-T6GBL is proposed to be analogous to that of lactone/lactide monomers (Scheme 3), in which slow initiation and cyclization relative to propagation allows the formation of the macrocyclic polyester.^{11,26}

2.3. Polymer thermal properties

Thermal stability of linear and cyclic P(4,5-T6GBL) was compared by TGA, using samples of similar M_n (~ 40 kDa). An additional sample of linear polymer (~ 20 kDa) was prepared using $\text{Ph}_2\text{CHCH}_2\text{OH}$ as the initiator to make a direct comparison to the polymers prepared by metal catalysts and analyzed in a previous study,³⁶ which used this initiator and M_n . Cyclic P(4,5-T6GBL) showed a T_d nearly 20 °C higher than the linear polymer in the case of metal-catalyzed ROP ($T_d = 323$ and 304 °C, respectively).³⁶ On the other hand, the cyclic and linear P(4,5-T6GBL) samples of ~ 40 kDa M_n by the current O-ROP method exhibited the same T_d of 317 °C (Fig. 4). The T_d of the linear P(4,5-T6GBL) prepared with $\text{Ph}_2\text{CHCH}_2\text{OH}$ initiator and $M_n \sim 20$ kDa for direct comparison was 13 °C higher than that of the polymer prepared with a metal catalyst (317 vs. 304 °C). The increased thermal stability of the sample prepared by O-ROP highlights another advantage of organocatalysis. This sample was also precipitated only one additional time after the initial precipitation of the crude polymerization, in contrast to three additional precipitations to remove any metal-based species when metal catalysts were used.³⁶ In this study, we also observed high polymer purity (no monomer or

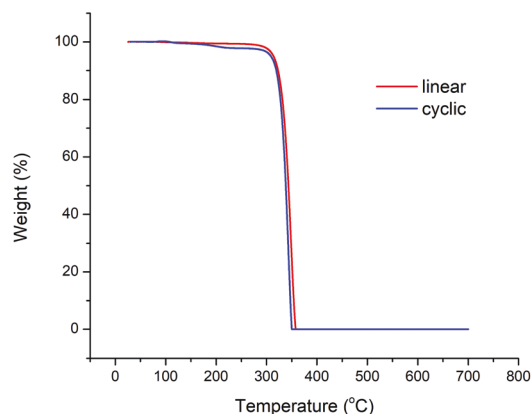


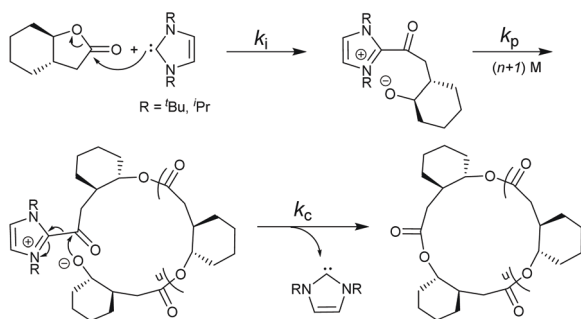
Fig. 4 TGA curves of linear and cyclic P(4,5-T6GBL) with $M_n \sim 40$ kDa produced by the current O-ROP.

catalyst peaks in NMR spectra) with only one total precipitation and copious washing of the polymer with cold methanol.

Polymer samples were also characterized by DSC analysis to locate the T_g for linear and cyclic polymers (Fig. S7 and S17[†]). The observed T_g 's of 74 and 75 °C for linear and cyclic samples, respectively, are in close agreement with the established values for P(4,5-T6GBL) (75 and 72 °C).³⁶ As expected, no melting transition was observed for these amorphous polymers. In addition, ^{13}C NMR spectrum of the linear polymer (Fig. S3[†]) exhibited multiple peaks for the carbonyl and stereogenic (β and γ) carbons, also indicative of an atactic polymer microstructure.

2.4. Organocatalyzed depolymerization

With the overarching goal of establishing a circular lifecycle for the P(4,5-T6GBL) material produced by the O-ROP method in mind, we investigated the organocatalyzed depolymerization of P(4,5-T6GBL). The TU-3/IMes pair, which was highly efficient in catalyzing the forward polymerization reaction, was not effective for the depolymerization. Only 8% conversion to monomer was observed after 24 h at 120 °C (0.4 M in toluene), but once again the *selective* nature of (T)U catalysts is highlighted. $t\text{Bu}$ was also found to be ineffective for depolymerization under the same conditions. TBD has been shown to catalyze the depolymerization of polyesters including P(GBL) and PET,^{21,32,33} and proved to be successful for the quantitative and selective depolymerization of P(4,5-T6GBL) at 120 °C (Fig. 5). Realizing both the forward and reverse reactions were possible with TBD, we performed a full circle experiment with 100/5/1 $[M]/[TBD]/[\text{BnOH}]$. GPC analysis of an aliquot taken after equilibrium was reached showed the formation of the polymer with $M_n = 7.62$ kDa and $D = 1.06$. The reaction mixture at that point contained 57% polymer, 43% monomer, and unquenched catalyst; this mixture was subsequently heated to 120 °C and the depolymerization was 98% complete in just 2.5 h. We initially used high dilution conditions to drive the reaction, but the above findings show potential for a solvent-free reactive (vacuum) distillation setup to enable a continuous depolymerization operation.³⁵



Scheme 3 Proposed mechanism of NHC-catalyzed polymerization to cyclic P(4,5-T6GBL).

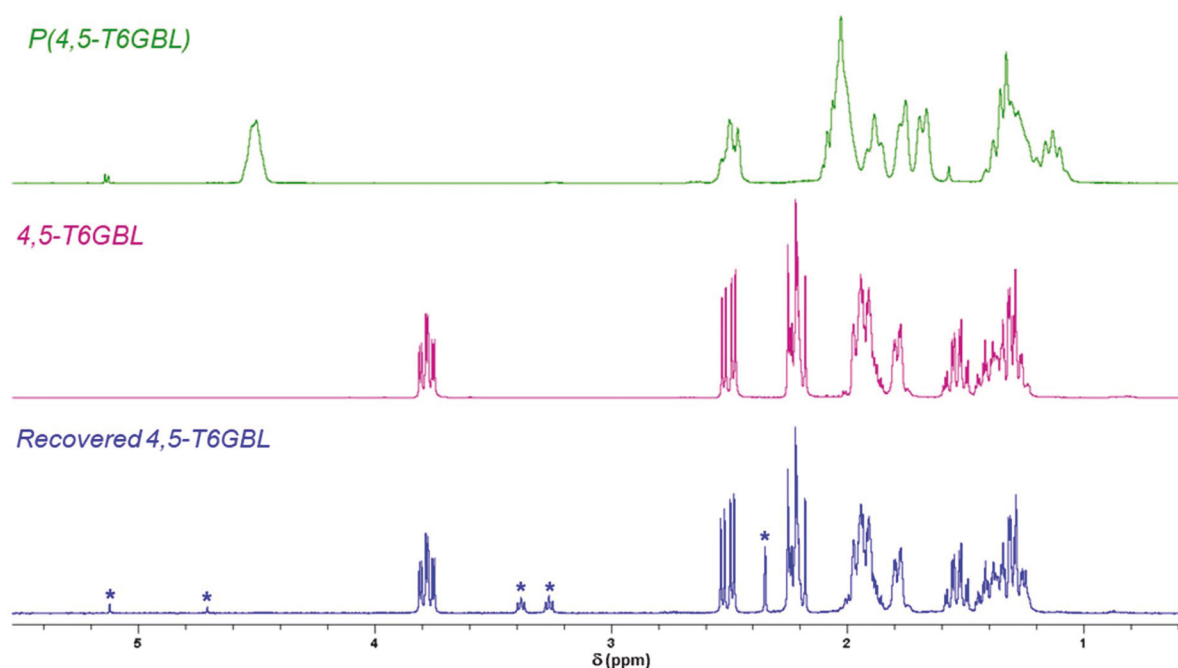
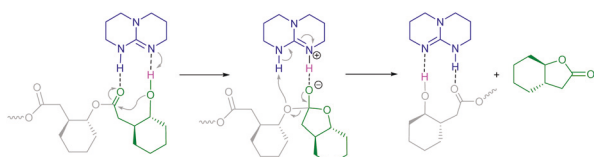


Fig. 5 NMR (CDCl_3 , 25 °C) spectra of starting polymer (top), starting monomer (center), and recovered monomer after depolymerization (bottom). Resonances marked with "*" for quenched TBD-H^+ , BnOH , and residual toluene.



Scheme 4 Proposed depolymerization mechanism catalyzed by TBD for the quantitative recovery of the stereo-retained monomer.

The mechanism of TBD-catalyzed depolymerization is proposed in Scheme 4, which is essentially a hydrogen bonding mediated cascade of backbiting reactions down the polymer chain, although some random chain scission may occur. First, the alcohol chain end must become activated through coordination to the basic nitrogen on TBD while the carbonyl of the same monomer unit is electrophilically activated by the acidic site, similar to the standard initiation mechanism of TBD.^{2,21} Next, the dual activation facilitates backbiting and subsequent formation of the thermodynamically stable GBL core of the monomer in a *trans* configuration. No formation of the less strained, more thermodynamically stable *cis* isomer was observed,⁴³ which occurs when $\text{P}(4,5\text{-T6GBL})$ undergoes thermolysis at 300 °C.³⁶ Upon formation of the lactone carbonyl bond, the formed monomer unit is released, and the catalyst regenerated.

3. Conclusions

In summary, we have established a convenient and effective method for the organocatalytic polymerization and depolymer-

ization of six-five bicyclic lactone 4,5-T6GBL. Linear polymers with M_n up to 106 kDa and low dispersity D of 1.04 can be selectively prepared using the optimal catalyst pair: 1,3-diisopropylthiourea (TU-3) and IMes, which are commercial reagents and were used with no further purification. The TU catalyzed polymerization exhibited living characteristics, as shown by predictable polymer M_n , low dispersity, kinetic profiling, NMR and MALDI-TOF chain end analysis, as well as the block copolymerization chain extension experiment. TU-3 combined with KOMe also catalyzed the polymerization and, under neat conditions, produced a polymer of $M_n = 137$ kDa in 6 h. TU-3 can also be combined with KH and MeOH, and this combination allowed the well-controlled bulk ROP to achieve high monomer conversion and produce $\text{P}(4,5\text{-T6GBL})$ with $I^* = 98\%$ and $D = 1.01$. Linear polymers prepared by the organic systems displayed less purification requirements and higher onset decomposition temperatures (>13 °C) as compared to those prepared with metal catalysts. Cyclic $\text{P}(4,5\text{-T6GBL})$ of $M_n > 40$ kDa can also be produced selectively by nucleophilic NHC catalysts. Guanidine base TBD was found to be effective in catalysing both polymerization and depolymerization of $\text{P}(4,5\text{-T6GBL})$. Depolymerization was both quantitative and selective in monomer recovery, with no isomerization to the *cis*-fused isomer.

Conflicts of interest

There are no conflicts to declare.

Acknowledgements

This work was supported by the United States National Science Foundation (CHE-1664915).

Notes and references

- 1 D. W. C. MacMillan, *Nature*, 2008, **455**, 304–308.
- 2 M. K. Kiesewetter, E. J. Shin, J. L. Hedrick and R. M. Waymouth, *Macromolecules*, 2010, **43**, 2093–2107.
- 3 C. Thomas and B. Bibal, *Green Chem.*, 2014, **16**, 1687–1699.
- 4 N. E. Kamber, W. Jeong, R. M. Waymouth, R. C. Pratt, B. G. G. Lohmeijer and J. L. Hedrick, *Chem. Rev.*, 2007, **107**, 5813–5840.
- 5 W. N. Ottou, H. Sardon, D. Mecerreyes, J. Vignolle and D. Taton, *Prog. Polym. Sci.*, 2016, **56**, 64–115.
- 6 S. Hu, J. Zhao, G. Zhang and H. Schlaad, *Prog. Polym. Sci.*, 2017, **74**, 34–77.
- 7 F. Nederberg, E. F. Connor, M. Möller, T. Glauser and J. L. Hedrick, *Angew. Chem., Int. Ed.*, 2001, **40**, 2712–2715.
- 8 A. P. Dove, R. C. Pratt, B. G. G. Lohmeijer, R. M. Waymouth and J. L. Hedrick, *J. Am. Chem. Soc.*, 2005, **127**, 13798–13799.
- 9 B. G. G. Lohmeijer, R. C. Pratt, F. Leibfarth, J. W. Logan, D. A. Long, A. P. Dove, F. Nederberg, J. Choi, C. Wade, R. M. Waymouth and J. L. Hedrick, *Macromolecules*, 2006, **39**, 8574–8583.
- 10 G. W. Nyce, T. Glauser, E. F. Connor, A. Möck, R. M. Waymouth and J. L. Hedrick, *J. Am. Chem. Soc.*, 2003, **125**, 3046–3056.
- 11 D. A. Culkin, W. Jeong, S. Csihony, E. D. Gomez, N. P. Balsara, J. L. Hedrick and R. M. Waymouth, *Angew. Chem., Int. Ed.*, 2007, **46**, 2627–2630.
- 12 M. K. Kiesewetter, M. D. Scholten, N. Kirn, R. L. Weber, J. L. Hedrick and R. M. Waymouth, *J. Org. Chem.*, 2009, **74**, 9490–9496.
- 13 J.-B. Zhu and E. Y.-X. Chen, *J. Am. Chem. Soc.*, 2015, **137**, 12506–12509.
- 14 X. Zhang, G. O. Jones, J. L. Hedrick and R. M. Waymouth, *Nat. Chem.*, 2016, **8**, 1047–1053.
- 15 B. Lin and R. M. Waymouth, *J. Am. Chem. Soc.*, 2017, **139**, 1645–1652.
- 16 B. Lin and R. M. Waymouth, *Macromolecules*, 2018, **51**, 2932–2938.
- 17 H.-Y. Ji, B. Wang, L. Pan and Y.-S. Li, *Angew. Chem., Int. Ed.*, 2018, **57**, 16888–16892.
- 18 H. Li, H. Luo, J. Zhao and G. Zhang, *ACS Macro Lett.*, 2018, **7**, 1420–1425.
- 19 M. Hong and E. Y.-X. Chen, *Angew. Chem., Int. Ed.*, 2016, **55**, 4188–4193.
- 20 A. Khalil, S. Cammas-Marion and O. Coulembier, *J. Polym. Sci., Part A: Polym. Chem.*, 2019, **57**, 657–672.
- 21 C. Jehanno, M. M. Pérez-Madriral, J. Demarteau, H. Sardon and A. P. Dove, *Polym. Chem.*, 2019, **10**, 172–186.
- 22 C.-J. Zhang, L.-F. Hu, H.-L. Wu, X.-H. Cao and X.-H. Zhang, *Macromolecules*, 2018, **51**, 8705–8711.
- 23 M. Li, Y. Tao, J. Tang, Y. Wang, X. Zhang, Y. Tao and X. Wang, *J. Am. Chem. Soc.*, 2018, **141**, 281–289.
- 24 L. Lin, D. Han, J. Qin, S. Wang, M. Xiao, L. Sun and Y. Meng, *Macromolecules*, 2018, **51**, 9317–9322.
- 25 B. Orhan, M. J. L. Tschan, A.-L. Wirotius, A. P. Dove, O. Coulembier and D. Taton, *ACS Macro Lett.*, 2018, **7**, 1413–1419.
- 26 H. A. Brown and R. M. Waymouth, *Acc. Chem. Res.*, 2013, **46**, 2585–2596.
- 27 S. Naumann and A. P. Dove, *Polym. Chem.*, 2015, **6**, 3185–3200.
- 28 P. Crotti, V. Di Bussolo, L. Favero, F. Macchia and M. Pineschi, *Tetrahedron Lett.*, 1994, **35**, 6537–6540.
- 29 M. Hong and E. Y.-X. Chen, *Green Chem.*, 2017, **19**, 3692–3706.
- 30 D. K. Schneiderman and M. A. Hillmyer, *Macromolecules*, 2017, **50**, 3733–3749.
- 31 D. J. Fortman, J. P. Brutman, G. X. De Hoe, R. L. Snyder, W. R. Dichtel and M. A. Hillmyer, *ACS Sustainable Chem. Eng.*, 2018, **6**, 11145–11159.
- 32 K. Fukushima, O. Coulembier, J. M. Lecuyer, H. A. Almegren, A. M. Alabdulrahman, F. D. Alsewailam, M. A. McNeil, P. Dubois, R. M. Waymouth, H. W. Horn, J. E. Rice and J. L. Hedrick, *J. Polym. Sci., Part A: Polym. Chem.*, 2011, **49**, 1273–1281.
- 33 M. Hong and E. Y.-X. Chen, *Nat. Chem.*, 2016, **8**, 42–49.
- 34 J. M. Eagan, J. Xu, R. D. Girolamo, C. M. Thurber, C. W. Macosko, A. M. LaPointe, F. S. Bates and G. W. Coates, *Science*, 2017, **355**, 814–816.
- 35 J.-B. Zhu, E. M. Watson, J. Tang and E. Y.-X. Chen, *Science*, 2018, **360**, 398–403.
- 36 J.-B. Zhu and E. Y.-X. Chen, *Angew. Chem., Int. Ed.*, 2018, **57**, 12558–12562.
- 37 J. Tang and E. Y.-X. Chen, *J. Polym. Sci., Part A: Polym. Chem.*, 2018, **56**, 2271–2279.
- 38 J. P. Brutman, G. X. De Hoe, D. K. Schneiderman, T. N. Le and M. A. Hillmyer, *Ind. Eng. Chem. Res.*, 2016, **55**, 11097–11106.
- 39 A. Rahimi and J. M. García, *Nat. Rev. Chem.*, 2017, **1**, 0046.
- 40 X. Zhang, M. Fevre, G. O. Jones and R. M. Waymouth, *Chem. Rev.*, 2018, **118**, 839–885.
- 41 X. Tang and E. Y.-X. Chen, *Chem*, 2018, **5**, 284–312.
- 42 *The new plastics economy: Rethinking the future of plastics*, World Economic Forum, Ellen MacArthur Foundation, and McKinsey & Company, 2016.
- 43 O. Haba and H. Itabashi, *Polym. J.*, 2014, **46**, 89–93.
- 44 A. Duda and A. Kowalski, in *Handbook of Ring-Opening Polymerization*, ed. P. Dubois, O. Coulembier and J.-M. Raquez, Wiley-VCH Verlag GmbH & Co. KGaA, Weinheim, Germany, 2009, pp. 1–51.
- 45 R. R. Walvoord, P. N. H. Huynh and M. C. Kozlowski, *J. Am. Chem. Soc.*, 2014, **136**, 16055–16065.